

## Motion of a polyelectrolyte chain hooked around a post

E.M. Sevick

*Department of Chemical Engineering, University of Colorado, Boulder, Colorado 80309-0424*

D.R.M. Williams\*

*Department of Physics, University of Michigan, Ann Arbor, Michigan 48109-1120*

(Received 18 July 1994)

The release kinetics of a single DNA molecule hooked around an obstacle in the presence of an electric field is investigated. A kinetic model which includes both electrical and stretching forces is introduced and used both in computer simulation and in the development of a simple analytic argument. These predict two regimes which depend on  $Y = N/\beta$ , where  $N$  is the number of chain segments and  $1/\beta$  is the dimensionless field strength. For short chains,  $Y < 1$ , the characteristic unhooking time scales as  $N^2$ , whereas for long chains,  $Y > 1$ , it scales as  $N$ . Without introducing post friction, the model is able to reproduce recent experimental observations.

PACS number(s): 87.15.-v, 82.45.+z, 36.20.Ey, 0.5.60.+w

Gel electrophoresis is one of the most widely used techniques for size-separating charged molecular chains such as nucleic acids or synthetic polyelectrolytes. The separation is achieved by driving the chains through a gel, usually agarose or polyacrylamide, by an external electric field. As a result of the field-driven mobility and the obstacles that the gel provides, small chains pass through the gel quickly while longer molecules move more slowly. For very long chains, e.g., DNA in excess of 30 kilobase pairs, the mobility has only weak dependence upon chain length, eliminating any possibility of separating very long chains. In a pulsed field, this saturation zone is postponed to larger chain lengths, but the mobility can also be nonmonotonic with chain length and can prevent a simple separation.

In an effort to understand and eventually to control the size-dependent mobility of electrophoresis, several researchers have concentrated upon dynamics of the simplest interaction between a chain and an obstacle in an electric field, i.e., a polyelectrolyte hooked upon a post [1-4]. Such hooking occurs when a chain, translating uniformly with the field, encounters an obstacle whose size is small in comparison to the size of the chain. The electric field rapidly unravels the coil on each side of the obstacle, forming a hairpin or a U shape (Fig. 1) [5]. The chain-length dependence of hairpin formation and hairpin release is an important model problem for the design of obstacle arrays which exhibit optimal electrophoretic separation.

In this Rapid Communication we model the release kinetics of a hooked polyelectrolyte chain taking account of both the electrical and chain stretching forces. Following the model dynamics using computer simulation and explaining the results with simplified analytic arguments, we are able to reproduce recent experimental results [2,4]. The polyelectrolyte is modeled as a chain of  $N$  freely jointed links of

length  $l$ , [6]. The chain is freely draining [7] and, for the stretched chains considered here, excluded volume effects can be neglected. The applied electric field is  $E$ , the effective charge per unit length is  $\lambda$  [8], and the temperature is expressed in Boltzmann units,  $kT$ . The dimensionless quantity  $\beta \equiv kT/(El^2\lambda)$  is the ratio of thermal to electrical energy for a single link. The quantity  $Y \equiv N/\beta$  describes the relative importance of the temperature and the field on the scale of one chain. We consider values for  $Y$  for which the chain is significantly distorted beyond its ideal radius,  $R_0 \sim l_r N^{1/2}$ . For  $N^{-1/2} < Y < 1$  the field stretches the chain considerably beyond this ideal radius but not to its fully stretched contour length,  $l_r N$ . This is the Gaussian or weakly stretched regime. For  $Y > 1$  the chain is close to its fully extended length. We then have the Langevin or strongly stretched regime.

Our model shows that inclusion of the stretching energy provides different chain-length dependences for the kinetics of hook unwinding in the regimes  $Y < 1$  and  $Y \gg 1$ , i.e., the weak and strongly stretched regimes. This is important as

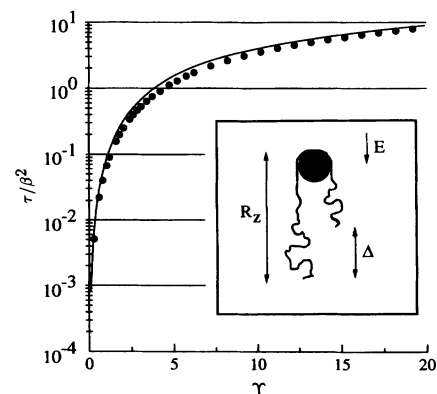


FIG. 1. Geometry of hooked polyelectrolyte (inset) and  $\tau/\beta$  versus  $Y = N/\beta$  where the points are simulation results for  $32 < N < 192$  with  $10 < \beta < 110$  and the line is the prediction of Eq. (8).

\*Permanent address: Institute of Advanced Studies, Research School of Physical Sciences and Engineering, The Australian National University, Canberra, Australia.

strong chain-length dependence is sought for size separation in electrophoresis. In addition, the predictions recover experimental results of chain and arm extension without invoking assumptions of static equilibrium [2]. Moreover, we find that the experimental chain unhooking [2] can be explained without invoking friction between the chain and obstacle. This is of importance as there has been some debate in the literature about post-chain friction [9].

Before investigating chain dynamics, it is instructive to examine the statics of a chain. Consider a polyelectrolyte chain of  $N$  segments in an electric field with one end,  $n=0$ , tethered to a point and the other end,  $n=N$ , free [10]. Let  $l_r z(n)$  be the upfield distance between the  $n$ th monomer of the chain and the tether point [11]. The free energy of the chain is written as

$$F = -\lambda E l_r^2 \int_0^N dn z(n) + kT \int_0^N dn S\left(\frac{dz}{dn}\right). \quad (1)$$

Here  $S(u) \equiv \int_0^u dv \mathcal{L}^*(v)$ , where the function  $\mathcal{L}^*$  is the inverse of the Langevin function,  $\mathcal{L}(x) \equiv \coth(x) - 1/x$ , so that  $\mathcal{L}^*(y) = 3y$  for  $y \ll 1$ , and  $\mathcal{L}^*(y) = 1/(1-y)$  for  $y \rightarrow 1$ . The first term in (1) is the electric potential energy, and the second term is the entropic free energy. This latter term describes the loss of entropy encountered whenever a chain is stretched [12]. For a uniformly stretched chain (which ours is not) the stretching energy reduces to the familiar Gaussian result,  $\frac{3}{2}kTR^2/(Nl_r^2)$ , where  $R = l_r z(N)$ , provided the degree of stretching,  $y \equiv dz(n)/dn$ , is less than about 0.5. However, in practice chains may be stretched somewhat more than this and the full Langevin elasticity, or its strong-stretching limit, must be used. In the strong-stretching limit  $y \rightarrow 1$ , the chain is almost stretched to its full contour length  $Nl_r$ , and the stretching energy becomes very large. Noting that  $z(n) = \int_0^n dp y(p)$  the free energy can be written in a more convenient form for analysis:

$$F/(El_r^2\lambda) = \int_0^N dn [(n-N)y(n) + \beta S(y)]. \quad (2)$$

The static or equilibrium trajectory of the tethered chain is obtained by taking the functional derivative of  $F$ ,  $\delta F/\delta y(n) = 0$ , which gives

$$y(n) = \mathcal{L}((N-n)/\beta). \quad (3)$$

This provides the stretching of the chain along its contour. Note that  $y$  has a maximum at the tether point,  $n=0$ , and that the stretching decreases monotonically from the tether point to the chain's free end. The extent of the chain in the field or  $z$  direction is found from  $R_z = l_r \int_0^N dn y(n)$  [10]. In the weakly stretched limit,  $Y < 1$ , the chain length has a strong dependence on the field,  $R_z = \frac{1}{6}l_r \beta^{-1} N^2$ ; and in the strongly stretched limit,  $Y \gg 1$ , we find  $R_z = Nl_r [1 - Y^{-1} \ln(2Y)]$ , i.e., the chain is almost fully stretched.

The dynamics of hairpin unwinding can now be found by equating the hydrodynamic drag on a segment moving at speed  $v$ ,  $A \eta l_r v$ , to the force on the segment

$$A \eta l_r^3 \frac{\partial z(n)}{\partial t} = - \frac{\delta F(z(n))}{\delta z(n)}, \quad (4)$$

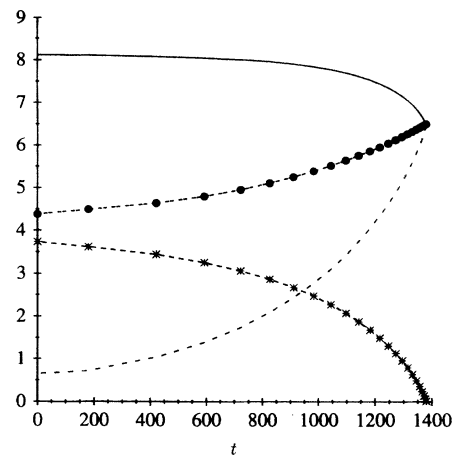


FIG. 2. Simulated chain extension, in units of link length, versus time for polyelectrolyte of  $N=100$  segments and dimensionless field  $\beta=100$ . Total extension of chain,  $z(1)+z(N)$ , (—); extension of advancing arm, (—●—); extension of retracting arm, (—\*—); difference in arm extension,  $\Delta = z(1) - z(N)$ , (· · · · ·). Simulated chain extensions for  $Y < 1$  and  $Y > 1$  show very similar behavior when scaled with maximum extent and unwinding time.

where  $\eta$  is the fluid viscosity,  $A$  a dimensionless drag constant, and the extra factors of  $l_r$  arise to render dimensional consistency. Inserting Eq. (1) into (4) yields

$$\tau_0 \frac{\partial z(n)}{\partial t} = \frac{1}{\beta} + \frac{\partial}{\partial n} \mathcal{L}^*\left(\frac{\partial z}{\partial n}\right), \quad (5)$$

where  $\tau_0 \equiv A l_r^3 \eta / (kT)$ . Brownian forces are neglected; as discussed below, they are unimportant, except at early times for hairpins with equal arm lengths. The hooking post is assumed to be a point that transmits the force between neighboring pivot segments, i.e., there is no friction between chain and post. The adopted initial condition is a hairpin with arms of  $N/2+2$  and  $N/2-2$  segments, with both arms set close to the equilibrium trajectory of a tethered chain (3).

A set of equations, consisting of Eq. (5) expressed for each  $n$ th segment  $2 < n < N-1$  and solved numerically over several time steps, forms the dynamic simulation. The simulation shows that at early unhooking time, the difference in length between the two arms,  $\Delta = z(1) - z(N)$ , is approximately exponential in time (Fig. 2) such that the unhooking dynamics can be expressed as  $d\Delta/dt = \Delta/\tau_c$ , where  $\tau_c$  is the characteristic unhooking time [4]. For the strongly stretched regime,  $Y > 1$ ,  $\Delta$  is purely exponential up until the final unhooking. Moreover, the total length of the chain  $z(1)+z(N)$  is constant throughout most of the unhooking dynamics, except towards the final unhooking. These simulation results coincide with the experimental observations in the strong-stretching regime [4]. Now consider the chain extension at late stages of the unhooking, i.e.,  $t > 1050$  in Fig. 2.  $\Delta$  is not a pure exponential; the total chain extension decreases noticeably; and the retraction of the short arm is much faster than the advance of the long arm (the retraction is exponential in time while the advance is linear). Each of these observations was found in the weak-stretching experiments of

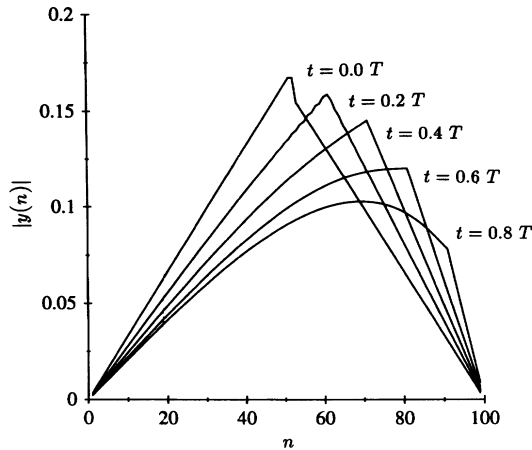


FIG. 3. Simulated stretching  $|y(n)|$  versus segment  $n$  along polyelectrolyte of  $N=100$  segments and dimensionless field  $\beta=100$  for various times,  $t=0.0T$ ,  $0.2T$ ,  $0.4T$ ,  $0.6T$ , and  $0.8T$  where  $T$  is the time for complete unwinding of the hooked chain from the obstacle. The initial stretching profile is set close to equilibrium stretching, Eq. (3). The pivot segment (where the derivative is discontinuous) advances along the contour of the chain until the chain “falls off” of the obstacle. The maximum stretching coincides with the pivot segment at early time, but lags behind the pivot at later times.

Song and Maestre [2] and these were interpreted correctly as being related to chain elasticity. However, in interpreting the faster retraction, Song and Maestre introduced friction at the pivot point and assumed that the stretching in the arms followed that of an equilibrium, tethered chain, Eq. (3). Neither friction nor a quasiequilibrium were required in the simulation to reproduce the experimental observations. Figure 3 demonstrates that the simulated chain departs markedly from two tethered, equilibrium arms. The discontinuity in the derivative of the stretching occurs at the pivot link of the chain. Note that as unhooking progresses, the maximum stretching occurs upfield of the pivot point, along the long arm, and not at the pivot point as (3) would suggest. Our frictionless model reproduces the experimental results without an additional equilibrium assumption of each of the arms. Friction is thus an unnecessary addition in describing the unhooking kinetics of experiments [9].

We now examine the dependence of  $\tau_c$  upon  $N$  and  $\beta$ . If the data are plotted as  $\tau_c/\beta^2$  versus  $Y=N/\beta$  all the points fall on a universal curve (Fig. 1). Two regimes are apparent: for  $Y < 1$ ,  $\tau_c \propto N^2$ , and for  $Y > 1$ ,  $\tau_c \propto N/\beta$ . For a fixed  $N$  the field strength dependence is as follows (Fig. 4): at high fields (small  $\beta$ )  $\tau_c \propto \beta^2$ , and at low fields (large  $\beta$ ),  $\tau_c$  approaches a constant.

The dependence of the characteristic time upon  $N$  and  $\beta$  can be understood from the following theory. Noting that the total extension remains constant for most of the unhooking time, changes in the stretching energy at early times are small in comparison to changes in electrical energy. Therefore we can neglect changes in stretching along the contour and approximate the tension at each point in the chain by its initial, equilibrium value, i.e.,  $|y(n)| = \mathcal{L}(n/\beta)$  for  $n < N/2$ ,  $|y(n)| = \mathcal{L}((N-n)/\beta)$  for  $n > N/2$ . The stretching of each

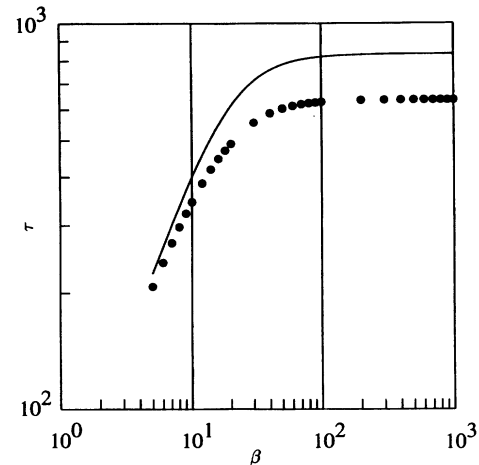


FIG. 4. The characteristic time  $\tau$  versus  $\beta$ . Simulation results for polyelectrolyte of  $N=100$  segments (●) and predictions of Eq. (8) (—).

segment is assumed invariant with time; however, the monomer position,  $P$ , of the pivot point and the electrical energy of the chain does change. Figure 2 shows that this is only an approximation, but our results (Figs. 1 and 4) indicate that the approximation is a good one. With this assumption, the total electrical energy of the chain is

$$\begin{aligned} \frac{F_e}{\lambda E l_r^2} = & \int_n^{N/2} dn(n-P) \mathcal{L}\left(\frac{n}{\beta}\right) + \int_{N/2}^P dn(n-P) \mathcal{L}\left(\frac{N-n}{\beta}\right) \\ & + \int_P^N dn(n-N+P) \mathcal{L}\left(\frac{N-n}{\beta}\right), \end{aligned} \quad (6)$$

where we have assumed  $P > N/2$ . The difference in arm extension (measured in units of  $l_r$ ) is

$$\Delta = \int_0^{N/2} dn \mathcal{L}\left(\frac{n}{\beta}\right) + \int_{N/2}^P dn \mathcal{L}\left(\frac{N-n}{\beta}\right) - \int_P^N dn \mathcal{L}\left(\frac{N-n}{\beta}\right). \quad (7)$$

The unhooking dynamics of  $\Delta$  is found by equating the drag in moving the chain [13] to the free energy change

$$\frac{1}{2} AN \eta l_r^3 (d\Delta/dt) = -(dF/d\Delta) = -(dF/dP)(d\Delta/dP)^{-1}.$$

Evaluating the derivatives and expanding the result in a Taylor series about  $\Delta=0$  gives  $d\Delta/dt = 2\Delta/[\tau_0 \beta N \mathcal{L}(N/(2\beta))]$ . Thus at early times the decay will be exponential with time constant

$$\tau_c = \frac{1}{2} \tau_0 \beta N \mathcal{L}(N/(2\beta)) = \frac{1}{2} \tau_0 \beta^2 Y \mathcal{L}(Y/2). \quad (8)$$

This theoretical prediction of characteristic time,  $\tau_c$ , agrees well with the results of the dynamic simulation (Figs. 1 and 4) and experiments. This is particularly true for  $Y > 1$ . For  $Y < 1$  the time is overestimated slightly, since chain contraction can take place. Thus at  $Y < 1$  we find  $\tau_c = \frac{1}{12} \tau_0 N^2$ , i.e., the time constant depends on the square of the molecular weight and is independent of the field. For  $Y \gg 1$  we find

$\tau = \tau_0(\frac{1}{2}\beta N - 1)$ . This is similar to the linear relation found earlier [4], although we differ from [4] by a factor of 2 in the slope.

In the above we have examined the potential-driven motion of the arms. Random thermal forces causing diffusive motion of the arms have been ignored [4], as diffusion is generally not important, except at very short times. The diffusion constant for  $\Delta$  is  $D_{\text{dif}} = 2kT/(A\eta l_r N)$  and, without a potential, the distance diffused in time  $t$  is  $\Delta \sim \sqrt{Dt}$ . If we set  $t = \tau_c$ , then the distance diffused in one decay time for  $Y < 1$  is  $\Delta \sim l_r \sqrt{N/6}$ , i.e., about one ideal radius. This is

much smaller than the typical arm length  $\sim l_r N^2/\beta$ . In the strongly stretched regime the distance diffused is  $\Delta \sim l_r \sqrt{\beta}$ , again much less than an arm length  $l_r N/2$ . Thus in both cases diffusion is unimportant, unless we examine very early times for equal-armed hairpins.

E.M.S. acknowledges financial support from The Engineering Foundation, Research Initiation Grant. D.R.M.W. acknowledges financial support from the Donors of the Petroleum Research Funds, administered by the American Chemical Society, and from the NSF under Grant Nos. DMR-92-57544 and DMR-91-17249.

- 
- [1] J.M. Deutsch and T.L. Madden, *J. Chem. Phys.* **90**, 2476 (1989).
- [2] L. Song and M.F. Maestre, *J. Biomol. Struct. Dyn.* **9**, 87 (1991).
- [3] W.D. Volkmuth and R.H. Austin, *Nature (London)* **358**, 600 (1992).
- [4] W.D. Volkmuth, T. Duke, M.C. Wu, R.H. Austin, and A. Szabo, *Phys. Rev. Lett.* **72**, 2117 (1994).
- [5] Such hairpins also exist in nematic polymers but in that case their dynamics and statics are different; J.M.F. Gunn and M. Warner, *Phys. Rev. Lett.* **58**, 393 (1987); D.R.M. Williams and M. Warner, *J. Phys. (Paris)* **51**, 317 (1990); in *Computer Simulation of Polymers*, edited by R. J. Roe (Prentice Hall, Englewood Cliffs, NJ, 1991).
- [6] Note that the persistence length  $l_p = l_r/2$ .
- [7] F. Brochard-Wyart and P.G. de Gennes, *C.R. Acad. Sci. Paris, Ser. II* **307**, 1497 (1988).
- [8] Note that in [4] electro-osmosis is taking place so the effective charge is much greater than the actual charge.
- [9] S. Burlatsky and J. Deutch, *Science* **260**, 2476 (1989); J.L. Viovy and T. Duke, *ibid.* **246**, 112 (1994).
- [10] J.M. Schurr and S.B. Smith, *Biopolymers* **29**, 1161 (1990); S.B. Smith and A.J. Bendich, *ibid.* **29**, 1167 (1990).
- [11] In the regimes considered here, and in the experiments [2–4], the chain does not fluctuate appreciably from its mean trajectory, a situation encountered for instance in the theory of polymer brushes; A.N. Semenov, *Zh. Eksp. Teor. Fiz.* **88**, 1242 (1985) [*Sov. Phys. JETP* **61**, 733 (1985)].
- [12] P.J. Flory, *Principles of Polymer Chemistry* (Cornell, Ithaca, NY, 1953).
- [13] Note that the monomers move at *half* the speed of  $\Delta$ , thus there is a factor of  $\frac{1}{2}$  in the drag. We thus differ in the strong-stretching limit by a factor of 2 from the calculation of Ref. [4].